Session 3A6
Extended/Unconventionl Electromagnetic Theory, EHD/EMHD, and Electrobiology

Chasmas Including Magnetic Effects

D. K. Callebaut (University of Antwerp, Belgium); A. H. Khater (University of Beni-Suef, Egypt); 790

Generation of Solar Magnetic Fields Using a Quadripolar Seed Field

D. K. Callebaut (University of Antwerp, Belgium); 793

Higher Order Fourier Analysis for Multiple Species Plasma

D. K. Callebaut (University of Antwerp, Belgium); G. K. Karugila (Dept. of Biometry and Mathematics, Faculty of Science, Tanzania); A. H. Khater (University of Beni Suef, Egypt); 796

Significance of Electric Quadrupole in Laboratory, Atmospheric, and Space Electricity — Helicity and Vortex Generation, Particle Acceleration, and Electric Discharges

H. Kikuchi (Institute for Environmental Electromagnetics, Japan); 799

Accuracy of Air Ion Field Measurement

T. Vojtek (Brno University of Technology, Czech Republic); T. Skoupil (Brno University of Technology, Czech Republic); P. Fiala (Brno University of Technology, Czech Republic); K. Bartušek (Brno University of Technology, Czech Republic); 800

Experimental Verification of Active Traveling Wave Antenna

T. Obata (Gunma National College of Technology, Japan); R. Miyazaki (Gunma National College of Technology, Japan); H. Kikuchi (Institute For Environmental Electromagnetics, Japan); 804

Some Analogy between Negative Shunt Conductance in a Distributed Parameter Line Equivalent to Parametrically Amplifying Traveling-wave Antenna and Negative Resistance in an Equivalent Lumped Circuit of Esaki Diode

H. Kikuchi (Institute for Environmental Electromagnetics, Japan); 805

Chasmas Including Magnetic Effects

D. K. Callebaut
University of Antwerp, Belgium
A. H. Khater
University of Beni-Suef, Egypt

Abstract—In a plasma one has by definition quasi-neutrality over distances of the order of the Debye length. In some situations one has no quasi-neutrality over many times the Debye length. Such a non-quasi-neutral plasma or charged plasma has been called chasma. We studied previously fairly simple chasmas [1–5] using an integro-differential equation and using the partial differential equations [6], where we obtained the so called 'chasma frequency', playing a role in the steady state and in the stability. Now we extend the latter analysis by considering the Maxwell equations from the start, i. e., including the magnetic terms. According to the geometrical situation (electron and ion velocities perpendicular to the 'electrodes' or not) one may derive expressions for all steady state quantities. Perturbation yields instability except in special cases, as was the case in the non-magnetic situation.

1. Introduction

In a plasma one has by definition quasi-neutrality in volumes which have dimensions larger than the Debye length or at least a few times the Debye length. In some situations one has no quasi-neutrality over many times the Debye length. E. g., in certain discharges or in the multipactor effect [1] (secondary electron resonance discharge) in the cavities of linear accelerators. It is expected that chasma's occur too in certain extended double layers with currents and magnetic fields playing a role in the solar convective zone and solar atmosphere or in double layers in the terrestrial atmosphere. Callebaut and Knuyt [2] investigated theoretically the steady state, using an approach based on a singular integro-differential equation, cf. [3–5] and [7–13] as well.

Here we want to analyze a fairly idealized situation, although not unrealistic in view of the studies cited above, however now using the basic partial differential equations. The study made in [6] did not involve a magnetic field, which was an inconsistency as currents were allowed to flow. Including the Maxwell equations complicates the system very much. For the steady state this is still no big problem. However, the investigation of the (linear) stability is more involved. In fact an extended quasi-nonneutral region requires already a particular configuration and circumstances to allow for an equilibrium, or rather a steady state. Thus it may be expected often to be unstable. Actually, observations in linear accelerators and in separated cavities seemed to indicate sometimes a stable behavior and sometimes an unstable one, although the latter might have been caused in some cases by exhaustion of the power supply.

2. Basic Equations

We have three sets of basic equations.

2.1. Maxwell Equations and Material Equations

With conventional notations we have

$$rot\mathbf{H} = \mathbf{j} + \partial_t\mathbf{D} = e(n_+\mathbf{v}_+ - n_-\mathbf{v}_-) + \epsilon\partial_t\mathbf{E}, \tag{1}$$

$$div\mathbf{B} = 0, \quad \to div\mathbf{H} = 0, \tag{2}$$

$$rot\mathbf{E} = -\partial_t\mathbf{B} = -\mu\partial_t\mathbf{H}, \tag{3}$$

$$div\mathbf{D} = \rho_+ + \rho_-, \quad \to \epsilon div\mathbf{E} = e(n_+ - n_-), \tag{4}$$

where we have inserted the material equations: $\mathbf{B} = \mu\mathbf{H}$ and $\mathbf{D} = \epsilon\mathbf{E}$. ϵ is the electric permittivity and equals in vacuum 8.85×10^{-12} C/Vm; μ is the magnetic permeability and usually is very close to its value in vacuum: $\mu = 4\pi \times 10^{-7}$ kgm/C (or henry/m), SI units. We assume that ϵ and μ are constant which is a reasonable hypothesis as it will turn out that we shall deal for the steady state with a homogeneous density; however, as some other quantities are varying in space an extension may be to have ϵ in tensorial form. The charge density of the electrons is ρ_-, their number density is n_-, their velocity is $\mathbf{v}_-$, their charge is $-e$ and their mass is m_-. For the ions, supposed ionized once only and all of the same mass, the same notation applies, but with a +sign replacing everywhere the -sign.

2.2. The Equations of Motion

With an obvious notation we have

$$n_\pm m_\pm \mathbf{v}_\pm.\nabla\mathbf{v}_\pm = \pm e n_\pm \mathbf{E} + \pm\mu e n_\pm \mathbf{v}_\pm \times \mathbf{H}. \tag{5}$$

These are the equations of motion for respectively ions and electrons in the cold plasma (chasma) approximation that the pressure terms are negligible.

2.3. Conservation of Charges (and Particles)

We express the conservation of charges, as well as the conservation of particles.

$$\partial_t \rho_\pm + \nabla.(\rho_\pm \mathbf{v}_\pm) = \pm P, \tag{6}$$

with P the ion charge density produced per unit time. Clearly there is a background of neutral particles that may get ionized by collisions. P is supposed here to be constant. P is usually the product of the beam density (here supposed to be constant), the density of the neutral gas and the ionization coefficient. In view of charge conservation during an ionization $-P$ corresponds to the electron charge produced per unit time and unit volume. In total we have 27 equations and 26 unknowns. After dropping $\mathbf{B}$, $\mathbf{D}$, $\mathbf{j}$, ρ_+ and ρ_- we still have 16 equations with 15 unknown functions. (The equations for the charge conservation and the equations (1) and (4) are not independent.)

3. Steady State

3.1. General

For the steady state we have $\partial_t = 0$ and thus the basic equations reduce to

$$\begin{aligned} rot\mathbf{H} &= e(n_+\mathbf{v}_+ - n_-\mathbf{v}_-), && (7)\\ div\mathbf{H} &= 0, && (8)\\ rot\mathbf{E} &= 0, \quad \rightarrow \mathbf{E} = -\nabla\varphi, && (9)\\ \epsilon\Delta\varphi &= -e(n_+ - n_-), && (10)\\ m_\pm \mathbf{v}_\pm.\nabla\mathbf{v}_\pm &= \mp e\nabla\varphi + \pm e\mu\mathbf{v}_\pm \times \mathbf{H}, && (11)\\ \nabla.(n_\pm\mathbf{v}_\pm) &= \pm P/e, && (12) \end{aligned}$$

where φ is the electric potential. We have omitted here for simplicity the index $_0$ for the steady state quantities. Note that e. g., $\mathbf{v}_{+0}$ and $\mathbf{v}_{-0}$ and φ_0 are still functions of space.

We consider the case of two infinite, plane-parallel plates ('electrodes') or infinite plane-parallel 'potential borders' of a double layer, which are far enough from each other so that we may neglect boundary effects. A homogeneous ionizing beam is creating electrons and ions while passing through the chasma region, either parallel to the plates or perpendicular to them. We choose the x-direction perpendicular to the plates and the y-direction parallel to them, along the beam if this one is parallel to the electrodes. The gradient of the potential is then in the x-direction. We have $\partial_y = 0$ and $\partial_z = 0$. The equations for the magnetic field yield

$$n_+ v_+ = n_- v_-, \tag{13}$$

$$\partial_x H_x = 0, \quad \partial_x H_y = 0, \quad \partial_x H_z = 0. \tag{14}$$

The total current has to vanish, i. e., the electron current compensates the ion current; otherwise there is no steady state. Moreover $\mathbf{H}$ has to be a constant field. It cannot be created by the chasma as there is no current, hence it is an applied magnetic field. Its orientation does not matter much as the charges moving in one place and deviated to another place replace other charges coming from elsewhere. For simplicity and with an eye on experimental situation we take $\mathbf{H} = \mathbf{H}_0$ either perpendicular or parallel to the electrodes.

Without an applied magnetic field, or when it is parallel to the velocities, the system of equations reduces to the one studied in our previous work [6], however, now with the supplementary relation (13). Note that this relation is rather natural as the same numbers of electrons and ions are generated in the ionization process, however, their densities are inversely proportional to their velocity, which suits equation (13) very well. (The fast back and forth sweeping h.f. beam, as e. g., in the multipactor effect, may be considered approximately as averaging to a zero current.)

3.2. Homogeneous Chasma

We know from the studies using the singular integro-differential equation [2–5] that steady states exist in which both n_+ and n_- are constant. Integration of the Poisson equation (10) yields then:

$$\varphi = -e\frac{(n_+ - n_-)x^2}{2\epsilon}, \tag{15}$$

where we have chosen the origin where the gradient of φ vanishes and omitted the arbitrary constant.

3.3. Beam Parallel to the Electrodes

With $\mathbf{v}_\pm \times \mathbf{H} = 0$ we recover the analysis given in [6]. As the production is usually proportional to the beam density, multiplied by an ionization frequency ω_{ch} we may write $P = \omega_{ch}\rho_{-0}$. There results

$$\omega_{ch}^2 = \frac{e^2(n_{+0} - n_{-0})}{\epsilon m_-}, \tag{16}$$

where we have called ω_{ch} the chasma (angular) frequency in [6]. It is a strange mix of the quantities constituting the electron and ion plasma frequencies. Moreover its meaning is different: this is an entity occurring in the steady state, and as such occurring in the stability analysis too, while the plasma frequency, although constituted by equilibrium quantities, appears in the perturbation analysis only.

4. Stability

The stability analysis of the chasma for the previous case is now much more involved than without current and magnetic field. Again there is mostly instability for some particular situations.

5. Conclusion

The present results using the full set of basic equations complement and confirm the result previously obtained with a singular integro-differential equation and the analysis in which the magnetic effects were neglected [6]. A constant beam and constant ion production leads to a homogeneous ion density and a potential quadratic in the coordinates. We introduced a so-called chasma frequency ω_{ch} which has a similar structure as the electron plasma frequency, but uses the difference in ion and electron number density instead of the equilibrium number density of either the ions or the electrons. Moreover its function is different. There is stability in particular cases, depending on ω_{ch} and the geometry.

REFERENCES

1. Callebaut, D. K., *Physica 29*, 784–802, 1963; *Physica 31*, 1177–1192, 1965; *Physica 32*, 1151–1158, 1966.
2. Callebaut, D. K. and G. K. Knuyt, *Phys. Lett. 29A*, 72, 1969; *Plasma Phys. 20*, 511–523, 1978; *Plasma Phys. 20*, 524–550, 1978; in *Relation between Laboratory and Space Plasmas*, (Ed. H. Kikuchi), Reidel Publ. Co., Dordrecht, The Netherlands, 207–230, 1981.
3. Callebaut, D. K. and G. J. Bex, *Workshop on Nonlinear Stability*, (Ed. D. K. Callebaut), UIA Press, University of Antwerp, Antwerp, Belgium, 154 & 161, 1989.
4. Callebaut, D. K., *Second URSI-ICPIG-RIKEN Symposium on Critical Problems of Discharge and Plasma Physics and Electro-Plasmo-Meteorology*, Riken (The Institute of Physical and Chemical Research), Wako, Saitama, 351-01, Japan, 40–41, 1995.
5. Callebaut, D. K. and A. H. Khater, *International Symposium on Nonconventional Plasmas*, (Eds. H. Kikuchi and D. K. Callebaut), Niigata, Japan, 1–2, 1997.
6. Callebaut, D. K., G. K. Karugila, and A. H. Khater, "Chasma perturbations," *Proc. PIERS 2005*, August 22–26, Hangzhou, China, 720–723, 2005.
7. Kikuchi, H., (ed.), *Relation between Laboratory and Space Plasmas*, Reidel Publ. Co., Dordrecht, The Netherlands, 1981.
8. Kikuchi, H., *Handbook of Atmospheric Electrodynamics*, H. Volland (ed.), CRC Press, Bonn, Vol. 1, 167, 1995.
9. Kikuchi, H., *Electrodynamics in Dusty and Dirty Plasmas (gravito-Electrodynamics and EHD)*, ASSL, Kluwer Acad. Press, Dordrecht, Vol. 258, 2001.
10. Schrittwieser, R. W. and G. Eder, (eds.), *Proc. Second Symposium on Plasma Double Layers and Related Topics*, Institut fr Theoretische Physik, Univ. of Innsbruck, A-6020 Innsbruck, Auqstria, 1984.
11. Schrittwieser, R. W., (ed.), *Fourth Symposium on Double Layers and Other Nonlinear Potential Structures in Plasmas*, (Innsbruck, Austria), World Scient., Singapore, 1993.
12. Verheest, F., M. Goossens, M. A. Hellberg, and R. Bharuthram (eds.), *Waves in Dusty, Solar and Space Plasmas, AIP Conference Proc.*, Leuven, Belgium, 537, 2000.
13. Verheest, F., *Waves in Dusty Space Plasmas*, Kluwer Acad. Press, Dordrecht, Vol. 245, 2000.

Generation of Solar Magnetic Fields Using a Quadripolar Seed Field

D. K. Callebaut
University of Antwerp, Belgium

Abstract—The exact solution for the kinematic dynamo problem in spherical coordinates r, ϑ, φ is given in Ref. 1. The velocity is supposed to be azimuthal and to be an arbitrary function of r and ϑ only. Using a bipolar seed field yielded a qualitative agreement with the sunspot butterfly diagram and the polar faculae butterfly diagram. Here we investigate the case that a quadripolar seed field resides in the Sun (maybe in the whole convective zone or rather only in the tachocline at the bottom of the convective zone). In fact some observations reveal a quadripolar contribution to some surface phenomena. A combination of a bipolar and a quadripolar field yields better agreement for a suitable choice of their amplitudes. The separation between the sunspot region and the polar faculae, although both are generated by the same mechanism, is manifest: the region where the radial variation of the angular frequency of the rotation vanishes.

1. Introduction

Here the dynamo is considered in the ideal magnetohydrodynamic (MHD) approximation: no resistivity and no α-effect. The basic equations are the equation for the evolution of the magnetic field $\mathbf{H}$ and the conservation of the magnetic flux

$$\partial_t \mathbf{H} = rot(\mathbf{v} \times \mathbf{H}), \tag{1}$$

$$div\mathbf{H} = 0, \tag{2}$$

where $\mathbf{v}$ is the velocity (SI units). The velocity field in the solar case may be assumed as being mainly a rotation around the solar axis (there is quite a good symmetry, sometimes a perfect anti-symmetry, with respect to the equator). Superposed on this main rotation are some turbulent motions, usually of much smaller amplitude. (Sometimes the turbulent speeds may be much higher, but they usually do not last long and alternate their direction.) They are not considered here, although their azimuthal component may be included in the treatment.

2. Exact Solution for Given Azimuthal Velocity

The system of spherical coordinates (r, ϑ, φ) is chosen so that the velocity $\mathbf{v}(r, \vartheta)$ has an azimuthal component only, v_φ. As only differential rotation matters (in our approach) for the amplification of the magnetic field this may be the differential velocity with respect to some chosen frame with uniform angular velocity, which is co-moving with some point e.g., on the equator. Hence

$$v_\varphi = r\omega(r, \vartheta) \sin \vartheta. \tag{3}$$

Here $\omega(r, \vartheta)$ is the angular frequency. Using the requirement that the magnetic field has to be single-valued Callebaut [1] obtained:

$$H_r = \frac{-1}{r^2 \sin \vartheta} \partial_\vartheta \Phi + P_r(r, \vartheta, \omega t - \varphi), \tag{4}$$

$$H_\vartheta = \frac{1}{r \sin \vartheta} \partial_r \Phi + P_\vartheta(r, \vartheta, \omega t - \varphi), \tag{5}$$

$$H_\varphi = \frac{-t}{r} \frac{\partial(\omega, \Phi)}{\partial(r, \vartheta)} + P_\varphi(r, \vartheta, \omega t - \varphi), \tag{6}$$

where the Jacobian is introduced. P_r, P_ϑ and P_φ are purely periodic functions of $\omega t - \varphi$, and contain r and ϑ in addition; they are related through the equations of flux conservation and field evolution. As one is essentially interested in growth with time and not in a periodic waxing and waning during one solar rotation, one does not bother much about the periodic terms P, although they may be relevant in connection with e.g., the mean field theory.

Φ is an arbitrary function of r and ϑ only. It follows from Eqs. (4) and (5) that H_r and H_ϑ do not vary with time except in their periodic terms. The only interesting time dependence (at present) is provided by the *linear* time dependence occurring as a coefficient of the Jacobian in H_φ. That the effective growth is linear with time may easily be understood physically. In fact the differential rotation tears the plasma, and the frozen-in magnetic field, differently in the φ direction, thus increasing H_φ. As the rotation is supposed steady, the increase is the same at all times, thus linear with time.

3. Quadripolar Seed Field

A contribution to the seed field consists of what is left over after part of the field has escaped at the solar surface. On the other hand there may be a part generated e.g., at the bottom of the convective zone. By lack of data on the seed field we have considered in [1] as an example a bipolar field. We gave there several arguments in favor of this choice: it is a fairly easy field, satisfying Eq. (2) and moreover planets have bipolar fields, although inside their field is far more complicated. Moreover this gave qualitatively good results. However, at the surface of the Sun, where huge currents encircling the Sun flow in filament bands, large-scale unipolar magnetic regions occur which yield a field with latitude bands of alternating signs (Callebaut and Makarov, 1992; Makarov, Callebaut, and Tlatov, 1997; Makarov et al., 2001; Makarov, Tlatov, and Sivaraman, 2003; Makarov, Tlatov, and Callebaut, 2002, 2005). Thus the choice of bipolar magnetic fields may be reasonable as a start, but one may be able to improve the results by using a combination of various types, e.g., a bipolar field together with a multipolar one. Moreover, we may consider the seed field to be in a shell only instead of in the whole region for $r > 0.7\,R$ with R the solar radius. Of course, the large and small scale turbulence and granular cells perturb the field continuously and so do the mechanisms loosing magnetic fields to space (sunspots, flares, polar faculae, bright points, coronal holes, ...) or to dissipation. We consider now the following quadripolar field separately (at first) as a tentative choice for the seed field:

$$H_r = r^{-4} H_p \cos\vartheta, \tag{7}$$

$$H_\vartheta = r^{-4} H_p \sin\vartheta, \tag{8}$$

in the region $r > R/2$ or rather $r > 0.7R$. The starting value for H_φ is irrelevant for the growth, however, it has to be independent of φ to make the field divergence vanish. H_p is a constant. It is clear that this initial field may be weak in general: to fix the ideas we may think of H_p/R^{-3}, the field at the equator, as a few gauss. However, in a narrow shell at the bottom layer of the convective zone the field may be thousands of gauss, even several hundred kilogauss. Of course, for the quadripolar field component the value may be much lower than for the bipolar one. (A combination of bipolar, quadripolar and octopolar seed fields will be envisaged later.) The components (7) and (8) may be matched to the expressions (4) and (5), which is an argument in favor for the choice of a bipolar seed field. The main difference with a bipolar field is that the latter has an r^{-3} dependence. We find

$$\Phi = -r^{-2} H_p \sin^2\vartheta. \tag{9}$$

4. Analytic Expression for the Differential Rotation

In [1] we obtained an approximate analytic expression for the angular frequency of the solar rotation per year:

$$\omega = \omega_{r_0} + \frac{5.77(r-r_0)(\cos^2\vartheta_0 - \cos^2\vartheta)(1+0.87\cos^2\vartheta)}{(R-r_0)\cos^2\vartheta_0}, \tag{10}$$

Here $\cos\vartheta_0 = 0.6$ is approximately the present value where $\partial_r\omega$ vanishes.

5. Growth

Using Eqs. (6), (9), and (10) we obtain

$$H_\varphi = \frac{5.77\,H_p t \sin\vartheta\cos\vartheta}{r^4(R-r_0)\cos^2\vartheta_0}\big[r(\cos^2\vartheta_0 - \cos^2\vartheta)(1+0.87\cos^2\vartheta) + 2(r-r_0)\sin^2\vartheta(1-0.87\cos^2\vartheta_0 + 1.74\cos^2\vartheta)\big]. \tag{11}$$

The formula is very similar to the one for a bipolar field: now r^{-4} appears as a factor instead of r^{-3} and a factor 2 in the second part of the formula. Proceeding with $r_0 = 0.7R$ (and $r_0 = 0.5R$ too, to see the influence) and $\cos\vartheta_0 = 0.6$ we obtain for H_φ and for X, the amplification factor per year, results similar to those obtained for the bipolar field.

1. Again we have very small growth in the region around latitude 37° or $\vartheta = 53°$. Here $\cos\vartheta = \cos\vartheta_0$ and $\partial_r\omega = 0$. Again for the latitudes in the vicinity of 37° there may be some growth of the field in one sense near $r = r_0$, while the growth is in the opposite sense near the solar surface $r = R$, resulting in a small total growth. This latitude band marks the separation between the equatorial region with sunspots and the polar region with polar faculae as $\partial_r\omega$ reverses sign.

2. Again there is no growth at the equator and at the poles. Again H_φ has opposite signs in both hemispheres. This suggests again that applying a time dependent seed field with period of about 22 years may be very suitable to explain the magnetic cycle (22 years) and not only the cycle of 11 years. However, as pointed out in [1], it is not a simple matter to explain the origin of such a time variation of the seed field.
3. An amplification of one order of magnitude is easily possible in some latitude bands. However, the growth rates are somewhat smaller than with a bipolar field. The general result matches qualitatively the sunspot butterfly diagram and the polar faculae butterfly diagram.

Using a combination of a bipolar and a quadripolar field may improve further the results by using appropriately chosen coefficients for both fields. This is a snag as we do not have an independent estimate of the relative ratios. However, from the observations of Makarov [7, 8, and 10] it may be possible to derive such an estimate, at least approximately. Similarly one may add an octopolar field with appropriate small coefficient, again in agreement with the observations of Makarov.

6. Conclusion

Growth rates of more than an order of magnitude during one solar cycle are easily possible in certain latitude bands when using a quadripolar seed field. We obtained, without using yet the α-effect, a qualitative correspondence for two of the main features of the solar activity depending on the latitude: the sunspot and polar faculae activities are explained by the same mechanism, but with some latitude gap between them due to the reverse of sign of $\partial_r\omega$ near latitude 37°. Making the bold (and still difficult to explain) hypothesis that the seed field oscillates with a period of 22 years would even allow to explain the magnetic cycle. Moreover, it turned out that the poleward migration of the circulation is not essential for the generation of the magnetic field.

The use of a quadripolar magnetic field as a seed field for the field generation in the solar dynamo seems plausible as an additional effect to the use of a bipolar field. One may even add a weak octopolar seed field. The appropriate ratios of bipolar, quadripolar and octopolar seed field may possibly be determined from certain observations on the solar surface. The use of a more involved dependence on the latitude than just $\sin^2\vartheta$ for Φ doesn't seem necessary. The main feature, the separation of the equatorial region with sunspots from the polar region with polar faculae, is mainly due to the fact that $\partial_r\omega$ reverses sign at a certain latitude (presently 37°) and not to the choice of the seed field.

REFERENCES

1. Callebaut, D. K., "Exact solution of simple kinematic dynamo," *Physica Scripta*, submitted.
2. Callebaut, D. K. and V. I. Makarov, "Latitude-time distribution of 3 types of magnetic field activity in the global cycle," *Solar Phys.*, Vol. 141, 381–390, 1992.
3. Callebaut, D. K. and V. I. Makarov, "Generation of sunspots and polar faculae from a kinematic dynamo," *Proc. Solar Phys.*, Meeting, SPM-11, 11–16, Louvain, Belgium, In press, Sept. 2005.
4. Makarov, V. I., A. G. Tlatov, and D. K. Callebaut, "Increase of the magnetic flux from polar zones of the sun in the last 120 years," *Solar Phys.*, Vol. 206, No. 2, 383–399, 2002.
5. Makarov, V. I. and D. K. Callebaut, *Solar Phys.*, submitted.
6. Makarov, V. I., D. K. Callebaut, and A. G. Tlatov, *Solar Phys.*, Vol. 170, 373–388, 1997.
7. Makarov, V. I. and V. V. Makarova, *Solar Phys.*, Vol. 163, 267–289, 1996.
8. Makarov, V. I. and V. V. Makarova, *Proc. 9th Eur. Meeting on Solar Phys.*, (ESA SP-448), 121–124, in A. Wilson (ed.), 1999.
9. Makarov, V. I., V. V. Makarova, and D. K. Callebaut, *Solar Phys.*, submitted.
10. Makarov, V. I., V. V. Makarova, and K. R. Sivaraman, *Solar Phys.*, Vol. 119, 45, 1989.
11. Makarov, V. I., A. G. Tlatov, D. K. Callebaut, V. N. Obridko, and B. D. Shelting, *Solar Phys.*, Vol. 206, No. 2, 383–399, 2002.
12. Makarov, V. I., A. G. Tlatov, and D. K. Callebaut, *Solar Phys.*, Vol. 224, No 2, 49–56, 2004.

Higher Order Fourier Analysis for Multiple Species Plasma

D. K. Callebaut
University of Antwerp, Belgium
G. K. Karugila
Dept. of Biometry and Mathematics, Faculty of Science, Tanzania
A. H. Khater
University of Beni Suef, Egypt

Abstract—Several first order perturbations of moderate amplitude may easily occur together in nature in a small interval of time. Each separately leads to a family of higher order terms which may total a somewhat larger amplitude. However, all the nonlinear terms of all first order perturbations may lead for a certain phase to a very large and even a divergent result. A kind of bunching, concentration of the energy in a small phase interval, occurs. This may act as a trigger and explain sudden outbursts which occur in nature (e. g., in solar flares, CMEs, bright points, prominences, etc.), on Earth (interruption of power generators) and in the laboratory. Inducing several moderate perturbations in a quiet plasma (e. g., a Q-machine) may allow experimental verification of the theoretical convergence limit.

1. Introduction

The nonlinear Fourier method of Callebaut consists in concentrating on the family of higher order terms of a single Fourier term of the linearized analysis [1–3]. Thus we have obtained the higher order terms of plasma perturbations, gravitational ones, etc. In the simplest case of a cold plasma this resulted in obtaining an analytical expression for the higher order terms. This allowed to investigate the convergence of the series, which in this case is e^{-1} of the equilibrium density. For the cases without an analytical expression we developed a numerical-graphical method to obtain the convergence limit. Near this limit the total amplitude of the wave becomes very large. The convergence limit decreases with increasing pressure.

We made an attempt [5] to explain a baffling aspect of some plasmas, e. g., prominences, that remain quiet during weeks, even months, and then suddenly burst out in an explosion with no apparent reason. Now we add a powerful argument to the reasoning in [5]: several first order perturbations of moderate amplitude may easily occur together in nature in a small interval of time. Each separately leads to a family of higher order terms which may total somewhat larger amplitudes. However, all the nonlinear combination of all first order perturbations may lead for a certain phase to a very large and even a non-convergent result.

2. A Basic Result

The nonlinear Fourier analysis by Callebaut was developed in several papers [1–3]. In particular an analytic expression for the cold plasma case was developed [2].Consider a first order perturbation n_1 of the density with amplitude A: $n/n_0 = Ae^{i(\omega t+kx)}$ normalized to the equilibrium density, using conventional notations. The associated family for the density) reads

$$n/n_0 = \Sigma_{s=1}^{\infty} \frac{s^s}{s!} A^s e^{is(\omega t+kx)}. \tag{1}$$

Similar expressions are valid for the velocity, the potential and the pressure.

This analytic expression allows to calculate the convergence ratio: $A < e^{-1}$. This means that the amplitude of the first order term has to be less than 37 per cent of the equilibrium density. Otherwise the associated sum, i.e., the full perturbation, diverges for at least one phase.

3. Several First Order Terms

Two remarks are here in order. The first one is that the above analysis is in fact an ordinary Fourier analysis of a specific solution of the system of equations with specific initial conditions: A, ω, k (which are in fact given by the first order term). In that sense the Fourier analysis is mathematically safe, as long as some very general conditions are satisfied of which the main one is that the situation is periodic, which is the case for the cold plasma. Nonlinearity comes in only when considering more than one of such first order terms. In that case interference or mixing occurs between the various families. However, once the series (1) is known, the solution for the nonlinear situation follows immediately from the binomial theorem:

$$n/n_0 = 1 + \Sigma_{s=1}^{\infty} \frac{s^s}{s!} (Ae^{i(\omega t + kx)} + Be^{i(\mu\omega t + kx)} + Ce^{i(\lambda\omega + kx)})^s. \tag{2}$$

B and C are first order amplitudes like A. The factors μ and λ are introduced as the various perturbations have various frequencies; for simplicity we kept the same wavenumber k. The extension to any number of first order terms is obvious.

The second remark concerns the initial amplitude required to have a divergent series: for the case of a single first order term this amplitude has to exceed 37 per cent of the equilibrium density to yield an instability. This requires usually an extremely strong perturbation, only possible if an extraordinary (big) bang is applied to the plasma. The limit is lowered when pressure terms are included, but even 5 or 10 per cent of the equilibrium are strong first order perturbations. This was a weak point in our paper (5). In nature or in the laboratory you need practically a neighboring explosion or the application of a (sudden) very large perturbing field. Ordinary shocks may not be sufficient. however, the application is quite different when we consider several perturbations as illustrated in equation (2). Now it is the sum of $A + B + C + ...$ that has to reach 0.37 to have a diverging total sum for some phases. If in nature e. g., perturbation occur with amplitudes around 0.01 then some 37 of such perturbations may blow up the plasma once the phase is reached where the sum becomes divergent. This is not an impossible demand, especially as the perturbations do not have to be originally in phase or have their frequencies in a rational proportion. This may allow quite a delay before the instability sets in, a feature which suits many observations. See below: applications.

We have drawn figures for several values of the parameters A, B, C, μ, λ: $A+B+C$ varied from 0.05 to 0.4, μ and λ took values $2, 5, \sqrt{2}, \sqrt{10}$. We considered various orders: $s = 1, 3, 10, 100$. Here we put some conclusions

1. If the total sum of the amplitudes is smaller than about 0.2 then the difference between order 3, 10, and 100 is very small.
2. If the total sum of the amplitudes is greater than 0.2 but less than about 0.3 then the difference between order 10 and 100 is very small.
3. If the total sum of the amplitudes is near 0.35, then one sees some difference between order 10 and 100.
4. For a total sum of the amplitudes above 0.35 the difference increases more and more. Above 0.37 (or e^{-1}) the series diverges (except for very special cases like the one in the cosine development). Moreover, the total density becomes negative (total density becomes less than zero for some arguments, which is physically impossible); this confirms that the series is not convergent.
5. The calculation time (using pentium 4 computer) is reasonable up to order 100. However, the time increases for each wave which is added especially for high orders.
6. Starting from several small amplitudes one may reach a solitonlike behavior for a certain phase (either in time or in space) with a quite large amplitude, especially when the sum of the initial amplitudes approaches 37% of the initial density. As in nature several (many) small perturbations may occur more or less together, although they may be generated at different places, this phenomenon may be important.

4. Applications

We just mention a few aspects. We refer to our paper (9), of course now having in mind several perturbations of reasonable amplitudes instead of the very big one required there.

4.1. Solar Flares, Filament Bands, Bright Points and CMEs

E. g., for a solar flare to be initiated waves may come from all sides at all times and it may take a long time (days, weeks) before the limiting value for instability is reached. Moreover, the strip in which the instability is initiated is very narrow (a finite energy is bunched together into a narrow space). From that strip the instability may spread over the whole flux tube (e. g., anomalous resistivity may occur) and thus some time elapses between the ignition and the flash (typically a quarter of an hour)liberating a tremendous amount of energy from a magnetic flux tube.

The same applies to e. g., a so-called “bright point” near the solar surface. Note that several small perturbations may ignite a bright point and that several bright points may ignite a prominence.

4.2. Power Generators on Earth

It is well known that power generators may crack down due to some perturbation which was apparently too small to cause the instability. Cf. March 1989 when the whole state of Quebec, Canada, was a day without electricity due to a solar storm which caused a magnetic perturbation spreading to the Earth. Again those perturbations seem often too small to have such an effect, but adding all the higher order terms and all the various perturbations may yield instability.

4.3. Ball Lightning

The most baffling feature of ball lightning is that it involves one or two orders of magnitude more energy than what may be expected from its light emission; the corresponding stability is equally surprising, sometimes followed by a quiet evanescent phenomenon, sometimes followed by a strong explosion. In [5] we have attempted to explain the huge energy contained in ball lightning by waves of the type of equation (1), rotating (or moving back and forth), but peaked in a narrow phase band. Moreover the cases where an explosion happens may be due to the combination of several perturbations of moderate amplitude as explained above.

4.4. Experimental Suggestion

In some experimental setups like the Q-machine one obtains a quiet plasma during reasonable periods. One may attempt to reach the instability limit by applying a very strong (sudden) external field, as suggested in [2]. However it may be easier to apply several perturbations (e. g., of different frequencies) each requiring a smaller amplitude. Plasmas with heavy negatively charged ions (fullerenes attach electrons) and positive ions may be suitable for this as their frequencies are much lower than for ordinary plasmas. However, a snag is that some electrons do not attach, resulting in a three species plasma. We are developing the appropriate extension of our nonlinear theory for this multiple species plasma.

5. Conclusion

In [5] we argued that a first order term may have a whole family of associated higher order terms which for some phase all combine together to form a powerful wave which may act as a trigger causing instability. The weak point was that the first order term had to be already very strong. Now, we have shown that the combination of several moderate first order terms and their families can yield a very strong (even divergent) perturbation in a narrow phase strip, thus having the possibility to act as a trigger locally or in a neighboring configuration.

REFERENCES

1. Callebaut, D. K., "Lineaire en niet-lineaire perturbaties in hydro-, magneto- en gravitodynamica," *Journal of the Mathematical Society of Belgium-Simon Stevin 45*, 1–315, Ghent, 1972.
2. Callebaut, D. K. and G. K. Karugila, "Nonlinear fourier analysis for unmagnetized plasma waves," *Physica Scripta*, Vol. 68, No. 1, 7–21, 2003. "Nonlinear fourier analysis for unmagnetized multi-species plasma waves," *Canadian Journal of Physics*, Submitted; "Nonlinear fourier approach yielding high fields in ball lightning," *Eighth International Symposium on Ball Lightning (ISBL04)*, 3rd–6th August 2004, National Central University (NCU), Chung-Li, Taiwan, 38–43, 2004.
3. Callebaut, D. K., G. K. Karugila, and H. Kikuchi, "Nonlinear stability of a gravitating medium with cosmological constant," *Kuwait J. Sci. Eng.*, Vol. 31, No. 2, 33–45, 2004.
4. Callebaut, D. K. and N. L. Tsintsadze, "Heating of plasma by alfvén waves envelope," *Physica Scripta*, Vol. 50, No. 3, 283–289, 1994; "Linear and nonlinear interaction of electromagnetic waves with weakly ionized magnetized plasmas," *Physica Scripta*, Vol. 52, No. 5, 565–571, 1995.
5. Callebaut, D. K. and G. K. Karugila, "Powerful nonlinear plasma waves from moderate first order perturbations," in PIERS 2005, Hangzhou, China, (Ed. J. A. Kung), 724–728, 2005.
6. Kikuchi, H., in *Handbook of Atmosphere Electrodynamics*, Vol. 1, (Ed. H. Volland, CRC press, Bonn, 167, 1995.
7. Kikuchi, H., *Electrodynamics in Dusty and Dirty Plasmas (Gravito-Electrodynamics and EHD)*, ASSL, Vol. 258, Kluwer Acad. Press, Dordrecht, 2001.
8. Dijkhuis, G. C., (ed.), *Sixth International Symposium on Ball Lightning (ISBL99)*, August 1999, UIA (now CDE, UA), University of Antwerp, B-2610 Antwerp, Belgium, 1999.
9. Veselovsky, I. S., "Non-local mass ejection development and without magnetic reconnection, in multi-wavelength investigations of solar activity," *Proc. of IAUS 223*, A. V. Stepanov, E. E. Benevolenskaya, and A. G. Kosovichev (eds.), Cambridge University Press, G. B., 517, 2004.
10. Webb, D. F., "Coronal mass ejections and space weather, in multi-wavelength investigations of solar activity," *Proc. of IAUS 223*, A. V. Stepanov, E. E. Benevolenskaya, and A. G. Kosovichev (eds.), Cambridge University Press, G. B., 449, 2004.

Significance of Electric Quadrupole in Laboratory, Atmospheric, and Space Electricity — Helicity and Vortex Generation, Particle Acceleration, and Electric Discharges

H. Kikuchi
Institute for Environmental Electromagnetics, Japan

An electric quadrupole can be constructed by four metallic spheres or a pair of dipoles above a metallic plane by positive and negative voltage application, forming an electrically neutral point or an electric cusp and an electric mirror.

A dust particle placed in a cusp region formed by a quadrupole is led to entirely different two consequences, depending upon whether the background gas pressure is below or beyond the gas breakdown threshold, though electric field merging to the particle occurs for both cases, suddenly causing very high local electric fields around the particle, almost zero to infinity. For the former case, the particle goes to helical motion, accompanying acceleration-deceleration and reflecting back at a mirror point or further running beyond the mirror point. So that the quadrupole can become a source-origin of helicity or vortex generation purely electrically. For the latter case, a sequence of processes occurs, namely surface discharge and ionization around the particle, being followed by EHD shocks, critical ionization, streamer and leader elongation, discharge channel formation towards each pole, and eventual main discharge or return stroke as a result of dust-related electric reconnection followed by critical ionization [1].

Consequently, electric cusp-mirror and reconnection model described above offers a unified view of dust dynamics and discharge-ionization and is thought to be useful for our basic understanding of those phenomena.

It should be noted that direct observational evidence of electric cusp-reconnection model has been obtained from a statistical survey by field experiments accidentally during winter thunderstorms (1985–89) in a costal region of the Sea of Japan, indicating that natural cloud-to-ground strokes occur most likely in a cusp region on the ground with an initially low electric field where a sudden change of low to very high electric field, almost zero to infinity, could occur, while such a catastrophe never happens in other areas of initially higher electric fields (pp. 91–93 in [1]). In addition, rocket- and tower-triggered lightning experiments indicate indirect evidence of this model (pp. 86–91 in [1])We are now planning direct laboratory evidence of this model by using a “universal electric-cusp type plasma reactor” (pp. 93–94 in [1]).

REFERENCES

1. Kikuchi, H., *Electrohydrodynamics in Dusty and Dirty Plasmas*, Kluwer Academic Publishers, Dordrecht/The Netherlands, 2001.

Accuracy of Air Ion Field Measurement

T. Vojtek, T. Skoupil, P. Fiala, and K. Bartušek
Brno University of Technology, Czech Republic

Abstract—An analysis of the electric state of air shows the presence of various ion sorts. The therapeutic effect of negative high-mobility ions of proper concentration is known. This positive effect was observed in caves that are used for speleotherapy. This article presents the capability of methods for measuring ion concentration and for ion spectral analysis.

1. Introduction

Air ion concentration and composition belong to the frequently monitored parameters of the atmosphere [5]. Their influence on living organisms has been the subject of intensive studies. Earlier research has demonstrated the positive influence of light negative ions and air cleanness on human health. The Department of the Theoretical and Experimental Electrical Engineering of Brno University of Technology and the Institute of Scientific Instruments of the Academy of Sciences of the Czech Republic are involved in the research of ion field in office and living spaces. The objective is to increase the concentration of light air ions in these spaces. Another task is to set up a simulated therapy room, with conditions similar to speleotherapy caves. It sets the requirements for accurate measurement of ion field with good repeatability. The article deals with the design of gerdien tube and peripheral measuring devices. An optimal design is important for eliminating the inaccuracy of ion concentration measurement.

2. Measuring Method

Several methods are currently used to measure air ion fields: the dispersion method, the ionspectrometer method, the Faraday cage method, and the gerdien tube method, whose principle is shown in Fig. 1 d_1—inner electrode diameter, d_2—outer electrode diameter, l—length of gerdien tube, M—air flow volume rate, v—air flow velocity, e—elementary charge of electron, $\oplus$ positive air particle (ion), $\ominus$ negative air particle (ion). The gerdien tube consists of two electrodes. There is an electric field between the inner electrode (the collector) and the outer electrode. The field is imposed by voltage source U. Air ions flow from the fan through the gerdien tube. Negative ions in the electric field impact the collector, and the current produced is measured by a pA-meter. The current measured is proportional to air ion concentration.

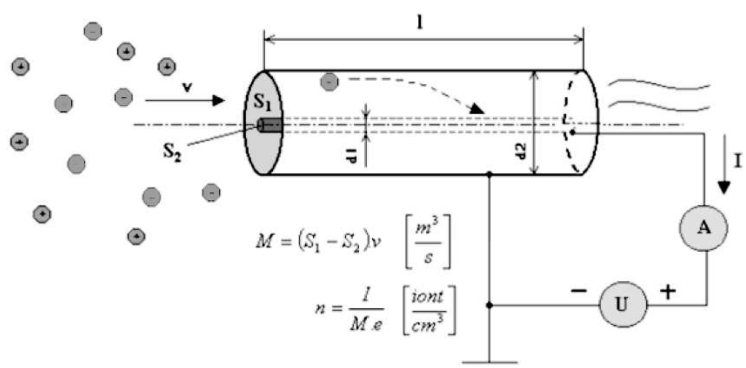

Figure 1: Principle of gerdien tube method.

The model of the measuring system is shown in Fig. 2. The values measured carry systematical measurement errors. This is due to leakage currents and parasitic capacitances (modeled by I_{LEAK} in Fig. 2) [6]. We have to consider leakage resistances R_{AK} of gerdien tube, leakage resistances and capacitance of the pA-meter input (R_{EH}, C_{EH}, R_{EL}, C_{EL}), insulation resistance (R_V) of the collector voltage source. The current measured is further affected by the input resistance of pA-meter and the input resistance of voltage source (R_U, C_U). To minimize the measurement error, R_{AK}, and R_V should be much larger than R_I, and R_{EH}, and R_{EL} should also be much larger than R_{OUT}. Time constant $R_U C_U$ has to be much larger than the measuring time.

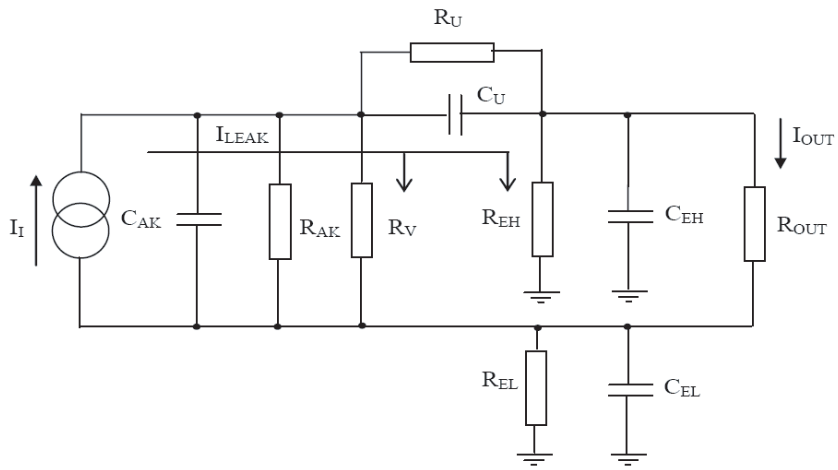

Figure 2: Model of a system for measuring air ion concentration—the gerdien tube method.

3. New Design of Gerdien Tube

The inner and outer electrodes are elliptical in shape. This shape ensures that the flow of air is laminar. Air flow turbulence can distort the accuracy of measurement. The surface of the electrodes is required to be as smooth as possible. These aspects make the design of gerdien tube quite demanding (fine grinding, lapping, etc.,). The new design of gerdien tube is shown in Fig. 3.

Since in the measurement of air ion concentration very small currents are detected, it is necessary to eliminate the influence of ambient electric charge. The influence of magnetic fields has to be minimized too.

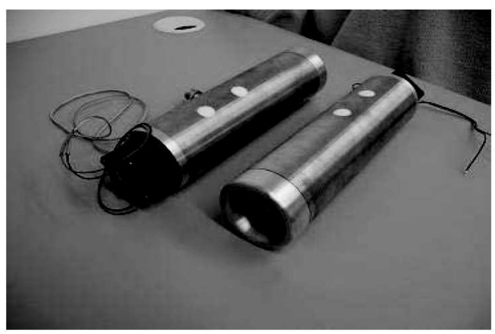

Figure 3: New gerdien tube.

4. Weak Current Amplifier

Table 1: Amplifier parameters.

I_{IN}	U_M	U_{out}	$Gain$	R_G
[pA]	[V]	[V]	[-]	[Ω]
0,1	1 m	1	1000	1 M
1	10 m	1	100	100 k
10	0,1	1	10	10 k
100	1	10	10	10 k

The current flowing through the gerdien tube consists of ions. Current intensity depends on polarization voltage, on the dimension and parameters of gerdien tube, and on ion concentration. The specific current range for the designed gerdien tube is 10^{-10} A–10^{-13} A.

For the following measurement it is suitable to convert the current to voltage. Because the current is very weak, it is suitable to do this near the gerdien tube. The transimpedance configuration is used for the conversion and amplification in the first stage.

The transimpedance amplifier is realized with an INA 116 opamp. The INA 116 has a very low input bias current $I_{b,max} = 100\,\mathrm{fA}$. The design of the amplifier is shown in Fig. 5. The first stage has transimpedance $R_T = 10\,\mathrm{G\Omega}$. The second stage is a variable-gain amplifier. The gain is set by resistor R_G. Table 1 shows the values of gain, voltage and current for various gain resistors. The resulting current-to-voltage conversion constant can be set to 0.1–1–10 pA/V.

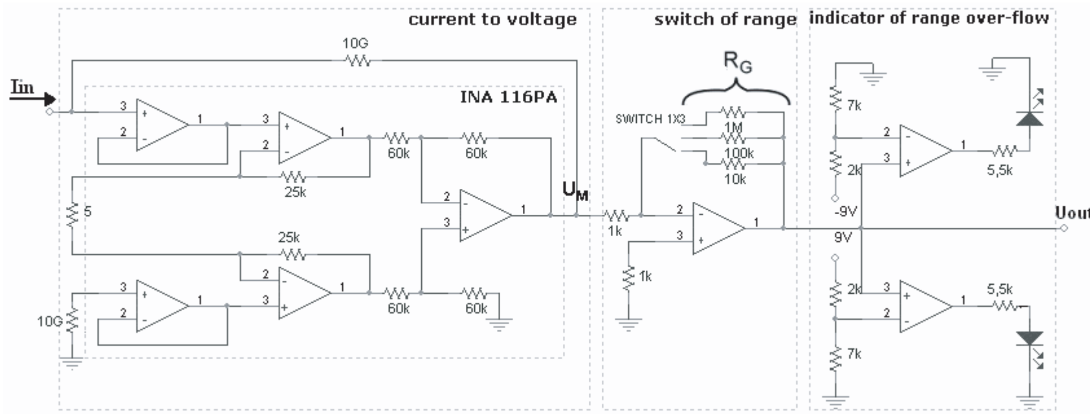

Figure 4: Design of pA-amplifier.

5. Comparison of Gerdien Tubes

The gerdien tube of new design was compared with two others. Gerdien tube configuration and parameters are shown in Figs. 5–7. Measurement results of tube are shown in Fig. 8.

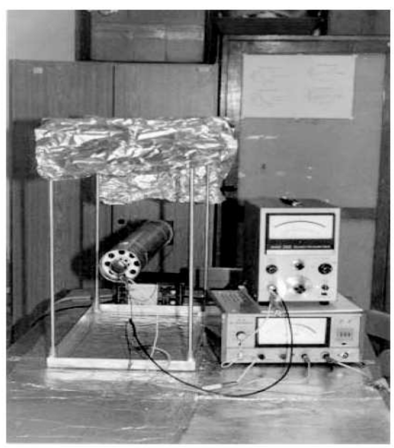

Figure 5: Gerdien tube [5].

$M = 10,62\,\mathrm{dm}^3$, $v = 4,3\,\mathrm{ms}^{-1}$, I_{leak}=0,4 pA @ 150 V

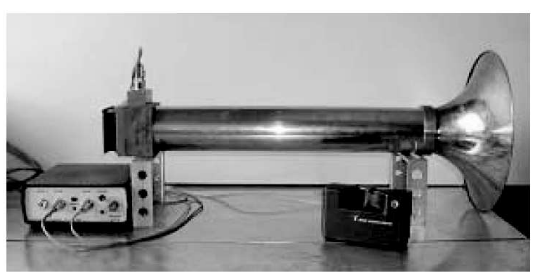

Figure 6: Gerdien tube [5].

$M = 12,14\,\mathrm{dm}^3$, $v = 3,75\,\mathrm{ms}^{-1}$, $I_{leak} = 0,3\,\mathrm{pA}$ @ 150 V

Figure 7: New design of gerdien tube.

$M = 0,75\ \mathrm{dm}^3$, $v = 0,8\ \mathrm{ms}^{-1}$, $I_{leak} = 0,05\,\mathrm{pA}$ @ $150\,\mathrm{V}$

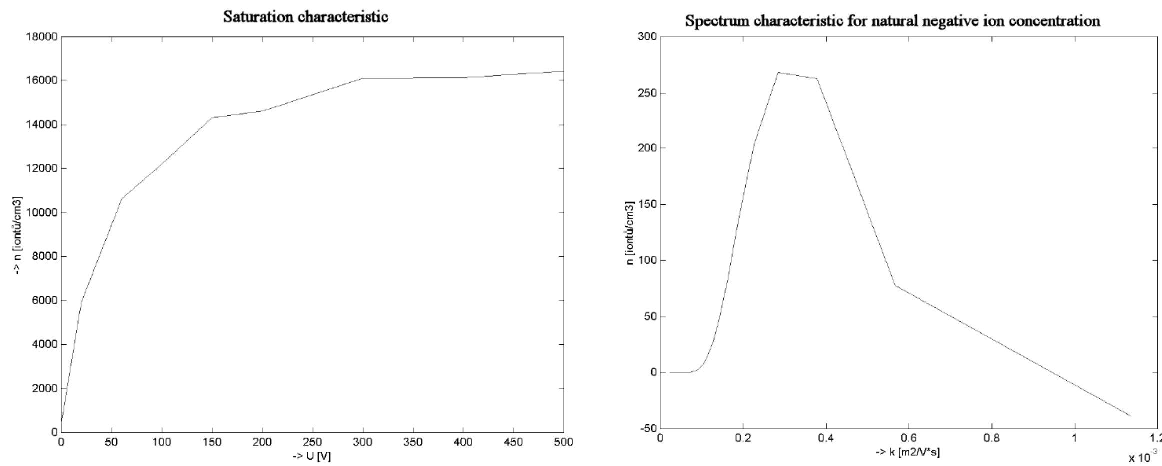

Figure 8: Results of measurment gerdien tube.

6. Conclusion

The new design of gerdien tube and the optimization of peripheral measuring devices have minimized the systematic error of measurement. The new system allows measuring air ion concentration with a sensitivity > 100 ions/cm^3. The ion mobility is in the interval 0.3–100 cm^{2}V^{-1}s^{-1}. The system will be used to measure ion field distribution in living and office spaces.

Very low leakage currents were achieved in the new design of gerdien tube. It allows higher sensitivity measurement. A long-term research task is to create an environment with suitable ion concentration and humidity in living spaces. The ion distribution in the environment will be simulated.

Acknowledgement

The paper was prepared within the framework of VUT Brno of the Czech Republic and with the support of the research plan MSM 0021630516.

REFERENCES

1. Bartušek, K., "Měření speleoterapeutických parametrů jeskyní pro lékařské účely," *Interní Text UPT AV ČR*, 1997.
2. Buřival, Z., "Vliv prostorového náboje v atmosféře na znečištění vzduchu v technologických provozech," *Knižnice Odborných a Vědeckých Spisů*, VUT Brno.
3. Spurný, Z., *Atmosferická Ionizace*, Praha, Academia, 1985.
4. Puškeilerová, L., "Nové poznatky o měření volných záorných iontů v laboratorním prostředí," Příspěvek k VŠTČ FEI, Brno 2000.
5. Israël, H., *Atmosphärische Elektrizität*, Akademische Verlagsgesellschaft Leipzig, 1957.
6. Smutný, T., "Vliv obvodových prvků na přesnost měření iontových polí," *Diplomová Práce*, VUT Brno, 2004.
7. Kafka, V., "Saturační a spektrální charakteristika iontového pole," *Diplomová Práce*, VUT Brno, 2004.

Experimental Verification of Active Traveling Wave Antenna

T. Obata[1], **R. Miyazaki**[1], **and H. Kikuchi**[2]

[1]Gunma National College of Technology, Japan
[2]Institute for Environmental Electromagnetics, Japan

Experimental verification in the principle of a parametric amplifying traveling-wave antenna proposed by Kikuchi [1] is tried. Long ago Carson [2] and also Pollaczek [3] developed a theory in regard to wave propagation along a wire above a dissipative ground. The Carson-Pollaczek theory, however, is restricted to a low frequency range, because of neglecting displacement currents in the air and in the ground and also no effects of the dielectric constant of the ground on equivalent circuit parameters. Kikuchi [4] developed a new theory overcoming these defects in Carson-Pollaczek theory. The new theory showed that attenuation characteristics possess a maximum and a minimum, and this was demonstrated by field experiments. The theory predicted fast waves between the maximum attenuation frequency and the minimum attenuation frequency, too. However, experimental verification of the fast waves is insufficient still now, except for a preliminary experiment by Iwai [5]. After that Kikuchi [6] extended the theory in distributed passive parameter lines so as to cover distributed active parameter lines with dissipative-ground return exposed to an electromagnetic environment. He showed that wave propagation along a wire above a dissipative ground exposed to an external electromagnetic field could be reduced to an active dissipative distributed parameter line with active source elements and passive circuit parameters. This new theory in active dissipative distributed lines predicted a new effect of parametric amplification of the induced line wave by an incident sky wave due to strong coupling or resonance between both waves. This is achieved by making the phase velocity of the induced wave nearly equal to the front velocity of the sky wave along the wire under some conditions. The authors try to verify the fast wave characteristic and the parametric amplification effect by an experiment.

REFERENCES

1. Kikuchi, H., United States Patent, Patent No. 5469179, 1995.
2. Carson, J. R., *Bell. Syst. Tech. J.*, Vol. 5, 539, 1926.
3. Pollaczek, F., *Elek. Nachr. Tech.*, Vol. 3, 339, 1926.
4. Kikuchi, H., *Electrotech. J. Japan*, Vol. 2, 73, 1956.
5. Iwai, T, unpublished work, 1999.
6. Kikuchi, H., *Proc. 7th Int. Wroclaw EMC Symp.*, edited by D. J. Bem et al., 153, Wroclaw Tech. Univ. Press, Wroclaw, 1984.

Some Analogy between Negative Shunt Conductance in a Distributed Parameter Line Equivalent to Parametrically Amplifying Traveling-wave Antenna and Negative Resistance in an Equivalent Lumped Circuit of Esaki Diode

H. Kikuchi
Institute for Environmental Electromagnetics, Japan

Structure of parametrically amplifying traveling-wave antenna is a wire above a semiconducting or lossy dielectric base-plate [1] and its eigen-mode becomes a fast wave for a certain high frequency range where the shunt conductance of its equivalent distributed parameter line becomes negative [2]. This new result of identity of a negative shunt conductance and a fast wave-mode is most remarkable and is a necessary condition for the present antenna to operate.

On the other hand, the Esaki diode is characterized by a negative resistance of an equivalent lumped circuit and plays a significant role as a semiconductor device based on quantum-mechanical tunnel effects as is well known [3].

An induced wave current of the present antenna is a fast wave. Therefore, when it is illuminated by an incident plane wave and its front velocity along the line is adjusted to be equal to the phase velocity of the induced line wave, parametrical amplification of the induced wave current along the line could be expected as a result of synchronization of both waves, thus the part of incident wave energy being transferred to the induced wave. In this way, the present antenna holds a high gain and a high directivity.

At low frequencies, however, the shunt conductance becomes positive, virtually being reduced to the conventional Beverage antenna. This corresponds to a positive resistance in the diffusion-dominant region in the Esaki diode.

Comparison of the present antenna and the Esaki diode is made illustratively in terms of voltage-current characteristics and their causing effects and mechanisms: attenuation and phase characteristics for the present antenna and energy-level diagram for the Esaki diode.

REFERENCES

1. Kikuchi, H., "Parametrically amplifying traveling-wave antenna," UK Patent 2276985, 1996; US Patent 5469179, 1995; French Patent 9404020, 1997; Japanese Patent 2636164, 1997; German Patent 4411720, 2004.
2. Kikuchi, H., "Active distributed parameter lines with ground return," *Proc. 7th Int. EMC Wroclaw Symp.*, 153–162, Wroclaw Technical University Press, Wroclaw/Poland, 1984.
3. Esaki, L., *Phys. Rev.*, Vol. 109, 603, 1958.